AIP Journal of Applied Physics

Temperature- and electric-field-dependent domain structures and phase transformations in (001)-cut tetragonal Pb (Mg 1/3 Nb 2/3) 1 − x Ti x O 3 (x = 0.40) single crystal

R. R. Chien, V. Hugo Schmidt, L.-W. Hung, and Chi-Shun Tu

Citation: Journal of Applied Physics **97**, 114112 (2005); doi: 10.1063/1.1927288
View online: http://dx.doi.org/10.1063/1.1927288
View Table of Contents: http://scitation.aip.org/content/aip/journal/jap/97/11?ver=pdfcov
Published by the AIP Publishing

Temperature- and electric-field-dependent domain structures and phase transformations in (001)-cut tetragonal $Pb(Mg_{1/3}Nb_{2/3})_{1-x}Ti_xO_3$ ($x=0.40$) single crystal

R. R. Chien[a] and V. Hugo Schmidt
Department of Physics, Montana State University, Bozeman, Montana 59717

L.-W. Hung and Chi-Shun Tu
Department of Physics, Fu Jen University, Taipei, Taiwan 242, Republic of China

(Received 8 June 2004; accepted 14 April 2005; published online 6 June 2005)

Temperature- and electric (E)-field-dependent domain structures and phase transformations in a (001)-cut $Pb(Mg_{1/3}Nb_{2/3})_{0.6}Ti_{0.4}O_3$ (PMNT40%) single crystal have been investigated by polarizing microscopy and dielectric permittivity. The unpoled crystal has tetragonal phase domains (15–60 μm wide) with polarizations along [100] and [010], which are separated by 90° domain walls. They coexist with a small fraction of the monoclinic phase domains near 200 K. The tetragonal domains increase rapidly at the expense of the monoclinic domains as the temperature increases toward room temperature. This may account for the steplike dielectric anomaly in ε' from around 280 K. The whole crystal reaches the cubic phase near 464 K. The E-field-dependent domain structures at room temperature show a significant change near 11 kV/cm when the polarizations rotate to the tetragonal [001] (T_{001}) direction through the monoclinic phase. Microcrackings begin to develop near 12.5 kV/cm. The entire crystal becomes T_{001} monodomain near 33 kV/cm. After the E field is removed, the crystal does not reestablish the T_{100} and T_{010} macrodomains, but instead breaks up into tetragonal microdomains. © *2005 American Institute of Physics*. [DOI: 10.1063/1.1927288]

I. INTRODUCTION

High-strain ferroelectric (FE) single crystals $Pb(Mg_{1/3}Nb_{2/3})_{1-x}Ti_xO_3$ (PMNTx) and $Pb(Zn_{1/3}Nb_{2/3})_{1-x}Ti_xO_3$ (PZNTx) exhibit extremely large electromechanical coupling factor k_{33} (>94%), ultrahigh piezoelectric coefficient d_{33} (>2500 pC/N), a large strain level (up to ~1.7%), and low hysteresis.[1] Such high piezoelectric performance, which converts mechanical and electric energies, gives extremely promising applications in medical imaging, actuators, sonar, and accelerometers. The exceptional piezoelectric properties have been related to the existence of M_A-, M_B-, and M_C-type monoclinic (M) and orthorhombic (O) phases in the morphotropic phase boundary (MPB) region between rhombohedral (R) and tetragonal (T) phases.[2,3] The intermediate phases (M and O) have been found in both PMNTx and PZNTx, and strongly depend on titanium content, temperature, history, strength of external E field, and crystallographic orientation. In addition, tetragonal PMNTx single crystals have shown excellent properties for promising optical applications.[4] Physical properties such as their thermal phase stability and E-field poling effect in the PMNT crystals and the mechanism underlying them should be addressed and understood so that such materials can be reliably used in devices.

The discovery of the intermediate phases has opened a window for searching for the origin of high piezoelectric responses. However, whether the intermediate phases are intrinsic, or merely appear as stress-induced responses to forces exerted by neighboring R, T, and/or cubic (C) domains or regions is not yet clear. In addition, how do the intermediate phases play a role in phase transformations among R, T, and C as temperature or applied E field changes? In this paper, we have investigated thermal phase stability and how poling affects polarizations in a (001)-cut PMNT40% crystal. By using relations of crystallographic symmetry and optical extinction, polarizing microscopy is capable of revealing orientations of the polarizations and their corresponding crystal phases. For interpreting polarizing microscopy domain observation among various phases, a review of principles of optical extinction for the (001)-cut crystal can be found in Ref. 5.

II. EXPERIMENTAL PROCEDURE

The PMNT40% single crystal was grown using a modified Bridgman method and was cut perpendicular to the ⟨001⟩ direction. The Ti concentration x was determined by using the dielectric maximum temperature T_m, i.e., $x=(T_m+10)/5$, where T is in °C.[6] A variable-frequency Wayne–Kerr precision analyzer PMA3260A with four-lead connections was used to obtain dielectric permittivity with gold electrodes deposited by radio frequency sputtering. A Janis CCS-450 closed-cycle refrigerator was used with a Lakeshore model 340 temperature controller. The heating/cooling ramping rate was 1.5 K/min.

The domain structures were studied by means of a Nikon E600POL polarizing microscope with a crossed polarizer-analyzer (P/A) pair. A Linkam THMS600 heating/cooling

[a]Author to whom correspondence should be addressed; electronic mail: chien@physics.montana.edu

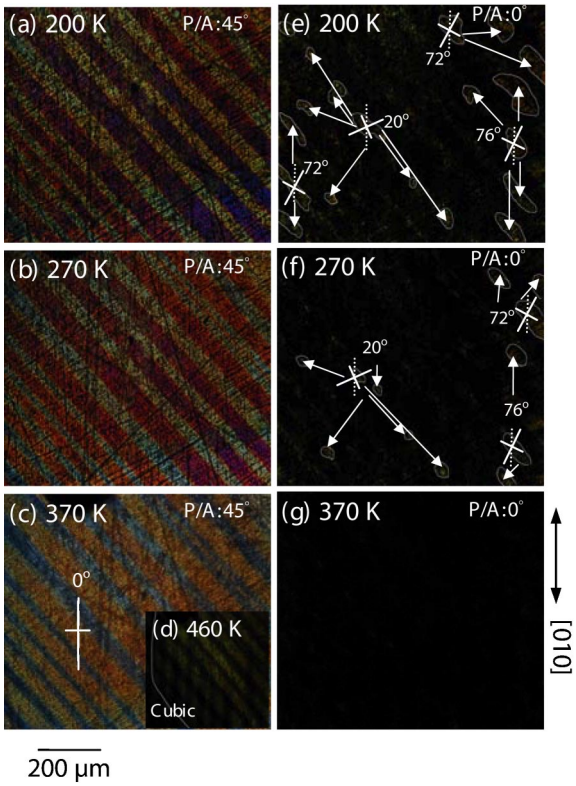

FIG. 1. (Color online) Temperature-dependent domain structures for the unpoled (001)-cut PMNT40% crystal.

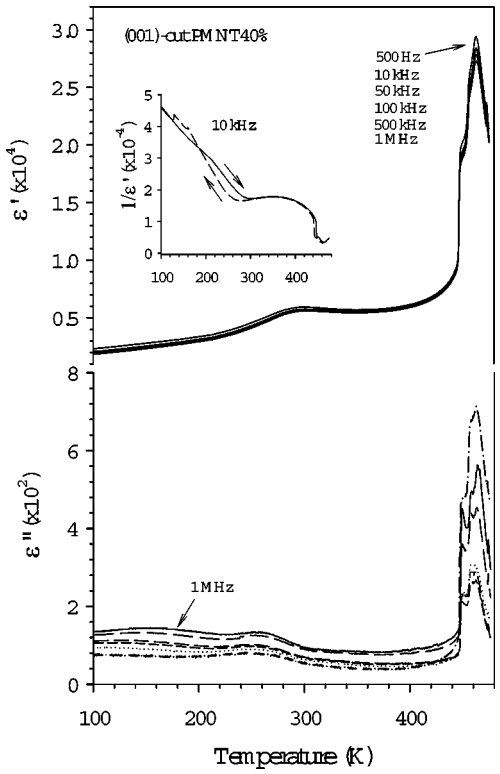

FIG. 2. Temperature- and frequency-dependent dielectric permittivities.

stage was mounted on the polarizing microscope for studying temperature-dependent domain structures. To minimize the superimposition of domains, the sample was polished to a thickness of about 45 μm. Transparent conductive films of indium tin oxide (ITO) were deposited on the sample surfaces for *E*-field-dependent domain observation. The experimental configuration for *E*-field-dependent domain observation can be found in the reference of Ref. 5. The crystal was annealed before all domain observations.

III. RESULTS AND DISCUSSION

A. Temperature-dependent domain observation

Before the zero-field-heating (ZFH) domain observation, the unpoled sample was cooled to 200 K after annealing. Figure 1 shows domain pictures of the unpoled (001)-cut PMNT40% crystal at various temperatures. Every angle expressed in the picture is the angle between one of the P/A pair axes and [010]. For instance, P/A: 45° in the upper right corner in the left column means that the domain picture was taken when the angle between one of the P/A pair axes and [010] was 45°. The angles 0°, 20°, 72°, and 76° appearing near the "cross" indicate that those domains exhibit extinction when the angles between one of the P/A pair axes and [010] are 0°, 20°, 72°, and 76°, respectively. As shown in Fig. 1(e), at 200 K most of the domain matrix exhibits extinction at 0°, i.e., one of the P/A axes is along the [010] direction. A small fraction of the domain matrix exhibits extinction at nonzero angles, such as 20°, 72°, and 76°. When observing the (001)-cut sample along the [001] direction between a crossed P/A pair, the extinction angle is $0°+m90°$ for all *T* domains, where *m* is any integer. We will measure all extinction angles in this work from the vertical direction, and will henceforth omit $m90°$ terms and only consider angles in the $0° \leqslant \phi < 90°$ range. Note that *O* domains also have extinction at 0°. However, if *O* domains exist in the sample, extinction would likely be seen also at 45°, which was not found in this study, as seen in Fig. 1(a), for 200 K. The extinction at 20°, 72°, and 76° corresponds to *M* or triclinic (tri) phases, which are indistinguishable in the polarizing microscopy. However, a tri phase has not yet been reported in PMNT crystals. Thus, the extinctions at 20°, 72°, and 76° most likely correspond to an *M* phase. As evidenced in Figs. 1(a)–1(c), the 15–60-μm-wide domains separated by 90° domain walls are dominated by *T* phase domains with polarizations **P** along the [100] and [010] axes (T_{100} and T_{010}). Therefore, it was evidenced that the dominant *T* domains coexist with a small fraction of *M* domains at 200 K. As the temperature increases, the *T* domains gradually increase from 200 to 270 K and rapidly increase above 270 K at the expense of the *M* domains, as seen in Figs. 1(f) and 1(g). This may account for the broad steplike anomaly in ε' near 280 K and the weak bump in ε'' near 260 K, as shown in Fig. 2. A similar broad steplike anomaly was also obtained near 200–210 K in our (001)-cut PMNT35% and PMNT38% crystals in the FR-ZFH process (poled at room temperature and then zero-field heated).[7] A long-range transformation of $T(M) \rightarrow T$ was evidenced from the polarizing microscopy and x-ray diffraction results.[7] $T(M)$ represents that dominant *T* domains coexist with a smaller fraction of *M* domains.

In addition, ε' and ε'' exhibit unexpected shoulders near 450 and 460 K (Fig. 2), which were not usually seen in other

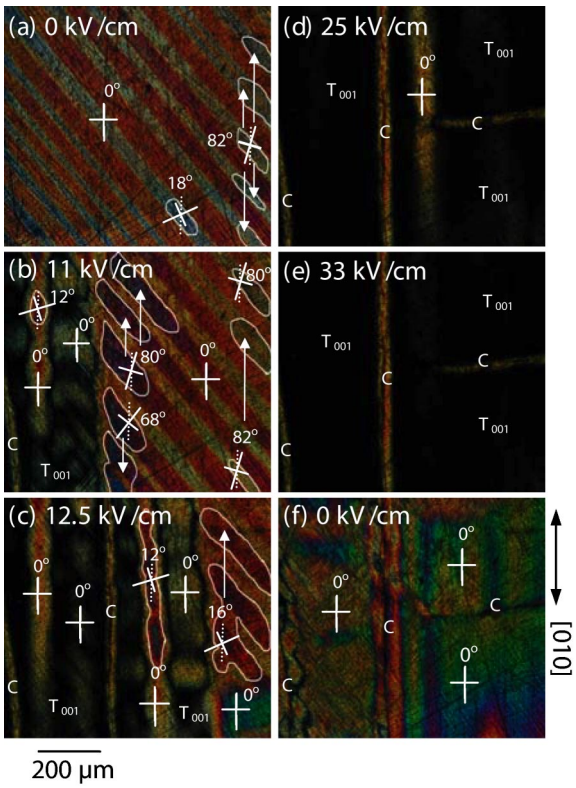

FIG. 3. (Color online) *E*-field-dependent domain structures at room temperature with a dc *E* field applied along [001]. The P/A angle was 45°.

close Ti concentration compounds, such as PMNT38% and 39%.[7,8] As evidenced in Fig. 1(d), some *C* phase regions appear near 460 K and expand throughout the whole crystal as the temperature increases gradually to 464 K, which is consistent with the dielectric maximum temperature T_m in Fig. 2. Therefore, the unexpected shoulders near 450 and 460 K most likely correlate to phase segregation that has often been seen in the PMNT system due to spatial heterogeneity of Ti content. Similar phase segregation was also observed in a (001)-cut PMNT29% crystal.[7]

B. *E*-field-dependent domain observation

The *E*-field-dependent domain structures, as shown in Fig. 3, were taken at P/A: 45° while a dc *E* field was applied along [001] at room temperature. At $E=0$ kV/cm [Fig. 3(a)], the domain matrix mostly exhibits an extinction at 0° and some at nonzero degrees such as 18° and 82° with respect to the [010] direction. This indicates the coexistence of a small fraction of *M* phase and a dominant *T* phase with polarizations **P** along the [100] and [010] axes. As the *E* field increases, the domain matrix does not essentially change until 11 kV/cm, as seen in Fig. 3(b). At $E=11$ kV/cm, the domain structure displays the T_{001} domain with polarization **P** along the [001] axis, which is associated with extinction at every orientation of the crossed polarizer/analyzer pair (i.e., total optical extinction), and some *M* domains with various nonzero-degree extinction angles, such as 12°, 68°, 80°, and 82° at the expense of the *T* domains. In other words, as the *E* field increases to 11 kV/cm, some of the *T* domains have transformed to T_{001} and *M* domains. With increasing *E* field [Fig. 3(c)], more of the *M* domains have been poled to the T_{001} domains, revealed by the total optical extinction, and the other *M* domains have changed their polarization orientations with various nonzero-degree extinction angles, such as 12° and 16°. Microcracking caused by the dc *E*-field poling process starts to develop at ~12.5 kV/cm along [010], as shown in Fig. 3(c), where *C*s indicate the cracks. As the *E* field increases to ~25 kV/cm [Fig. 3(d)], cracking along [100] appears and the entire domain matrix exhibits total optical extinction (i.e., the T_{001} domain) except a stripe oriented along [010]. The entire crystal becomes T_{001} monodomain near $E=33$ kV/cm, as seen in Fig. 3(e). However, a (001)-cut rhombohedral PMNT24% single crystal cannot reach a tetragonal monodomain and no microcracking was found under a higher *E* field (44 kV/cm) applied along [001] at room temperature.[5]

As the poling *E* field decreases from 33 kV/cm, the T_{001} monodomain does not exhibit apparent change until $E=12.5$ kV/cm. Then *T* domains with polarizations **P** along the [100] and [010] axes begin to appear at the expense of the T_{001} monodomain. After the *E* field was removed [Fig. 3(f)], the domain structure did not return to the broad T_{100} and T_{010} domains separated by the 90° domain walls [Fig. 3(a)]. However, the extinction pattern is in agreement with tetragonal microdomains with polarizations **P** along the [100] or [010] axes.

IV. CONCLUSIONS

In this study, it was evidenced that a few *M* phase domains coexist with the dominant T_{100} and T_{010} domains near 200 K in the unpoled (001)-cut PMNT40% crystal. These T_{100} and T_{010} domains are 15–60 μm wide and separated by 90° domain walls. As the temperature increases from 200 K to room temperature, the T_{100} and T_{010} phase domains increase rapidly at the expense of the *M* phase domains. The crystal reaches the *C* phase near 464 K. Instead of a $T\rightarrow C$ transition proposed for PMNT40% by the phase diagram,[2] a transition sequence of $T(M)\rightarrow T\rightarrow C$ was found. The *E*-field-dependent domain observation at room temperature found that T_{001} phase domains were induced near 11 kV/cm by the process (T_{100} or T_{010})$\rightarrow M\rightarrow T_{001}$, and this T_{001} phase expanded through the whole crystal by this process as the *E* field increased further. Microcracking phenomenon starts near 12.5 kV/cm. The crystal becomes entirely T_{001} monodomain near 33 kV/cm. After the *E* field was removed, the T_{100} and T_{010} macrodomains, and 90° domain walls cannot be obtained again. Instead, the crystal exhibits non-T_{001} tetragonal microdomains.

ACKNOWLEDGMENTS

The authors express sincere thanks to Dr. H. Luo and H. Cao for the crystal. This work was supported by DoD EPSCoR Grant No. N00014-02-1-0657 and NSC Grant Nos. 92-2112-M-030-007 and 93–2112–M-030–001.

[1] S.-E. Park and T. R. Shrout, J. Appl. Phys. **82**, 1804 (1997).
[2] T. R. Shrout, Z. P. Chang, N. Kim, and S. Markgraf, Ferroelectr., Lett. Sect. **12**, 63 (1990).
[3] B. Noheda, Curr. Opin. Solid State Mater. Sci. **6**, 27 (2002).

[4]C.-S. Tu, F.-T. Wang, R. R. Chien, V. H. Schmidt, and G. F. Tuthill, J. Appl. Phys. **97**, 064112 (2005).
[5]R. R. Chien, V. H. Schmidt, C.-S. Tu, L.-W. Hung, and H. Luo, Phys. Rev. B **69**, 172101 (2004).
[6]Z. Y. Feng, H. S. Luo, Y. P. Guo, T. H. He, and H. Q. Xu, Solid State Commun. **126**, 347 (2003).
[7]C.-S. Tu, R. R. Chien, F.-T. Wang, V. H. Schmidt, and P. Han, Phys. Rev. B **70**, 220103(R) (2004).
[8]R. Chien, V. H. Schmidt, C.-S. Tu, and L.-W. Hung, Ferroelectrics **302**, 335 (2004).